Article citation info:
Boutaybi M, Khlifi Y, Elhafyani ML. Performance comparison of classical and fuzzy logic MPPT techniques under sudden irradiation variations and their hardware implementation. Diagnostyka. 2025;26(3):2025312. https://doi.org/10.29354/diag/209196.



**DIAGNOSTYKA**, 2025, Vol. 26, No. 3

**e-ISSN** 2449-5220
**DOI:** 10.29354/diag/209196

# PERFORMANCE COMPARISON OF CLASSICAL AND FUZZY LOGIC MPPT TECHNIQUES UNDER SUDDEN IRRADIATION VARIATIONS AND THEIR HARDWARE IMPLEMENTATION

**Mohammed BOUTAYBI [1,*], Yamina KHLIFI [1], Mohamed Larbi ELHAFYANI [2]**

[1] Energy, Embedded System, and Data Processing Laboratory, National School of Applied Sciences Oujda (ENSAO), Mohammed First University (UMP), Oujda, 60000, Morocco
[2] Laboratory of Electrical Engineering and Maintenance, Higher School of Technology (ESTO), Mohammed First University (UMP), Oujda, 60000, Morocco
[*] Corresponding author, e-mail: mohammed.boutaybi@ump.ac.ma

Abstract

This study presents the simulation and experimental implementation of two distinct categories of Maximum Power Point Tracking (MPPT) algorithms aimed at optimizing the performance of Photovoltaic (PV) systems. The first category involves advanced Fuzzy Logic-based MPPT controllers, specifically FL-Mamdani and FL-Takagi Sugeno (FL-TS) models. These controllers utilize two input parameters: the gradient of the power-current curve and its variation, offering an alternative to conventional methods that depend on the gradient of the power voltage curve and its change. The second category consists of classical MPPT algorithms, including Incremental Conductance (IC) and Perturb and Observe (P&O). The experimental setup comprises a PV system with a TDC-P50-42 solar panel powering a resistive load through a boost converter. The converter's Mosfet is controlled via a Pulse Width Modulation (PWM) signal generated by the MPPT controller. The algorithms were first simulated using MATLAB/Simulink and then implemented in real-time using an Arduino board supported by the Simulink hardware package for Arduino. Experimental results confirm the proper functioning of the proposed PV system. Among the tested techniques, the FL-TS fuzzy logic controller demonstrated superior performance and reliability, validating its practical applicability in real-world PV applications.

Keywords: Arduino board; fuzzy logic; FL-TS; FL-Mamdani, MPPT

**List of Symbols/Acronyms**
CE: Change Of Error
D: Duty Cycle
E: Error
FL: Fuzzy Logic
FL-Mamdani: Fuzzy Logic Mamdani
FL-TS: Fuzzy Logic-Takagi Sugeno.
IC: Incremental Conductance
MPP: Maximum Power Point
MPPT: Maximum Power Point Tracking
MFs: Membership Functions
PWM: Pulse Width Modulation
PV: Photovoltaic
P&O: Perturb and Observe
$I_{pv}$ : Photovoltaic current
$I_{mpp}$: Current at the maximum power point
$V_{pv}$ : Photovoltaic voltage
$V_{mpp}$: Voltage at the maximum power point
STC: Standard Test Conditions.

## 1. INTRODUCTION

Due to its inherent advantages being free, renewable, and virtually limitless solar energy stands out as a highly promising and attractive energy source. In recent years, PV systems have received increasing attention owing to their wide range of applications, particularly in areas lacking access to electricity. These include water pumping systems [1-2], standalone photovoltaic installations [3-5], and more recently, solar-powered standalone charging stations for electric vehicles [6-8].

In a system where a PV panel is directly connected to a load, the operating point can lie anywhere along the power voltage P(V) curve and does not necessarily coincide with the Maximum Power Point (MPP). This mismatch often leads to system oversizing and reduced energy utilization efficiency, thereby increasing overall costs. The core challenge stems from the dynamic nature of the MPP, which continuously shifts due to changing weather conditions and variations in the connected load. As a result, ensuring efficient power extraction under varying levels of solar irradiance and temperature is essential, especially considering the relatively high cost of solar energy. To overcome this issue, the implementation of a MPPT control strategy is vital [9-10].

Received 2025-12-01; Accepted 2025-08-05; Available online 2025-08-17

A typical regulated photovoltaic system consists of connecting a PV panel to a load via a boost converter, which is controlled by MPPT algorithm. Numerous MPPT techniques have been proposed, experimentally validated, and analysed in various published research works [11-13].

The most commonly used MPPT algorithms in PV applications include classical methods such as Perturb and Observe [14-16] and Incremental Conductance techniques. These approaches are widely chosen due to their simplicity, ease of implementation, and the fact that they do not require prior knowledge of the PV system's characteristics [17-20].

However, the P&O algorithm suffers from several limitations, such as oscillations around the MPP, slow tracking response, and inaccurate MPP estimation under rapidly changing irradiance, temperature, or load conditions [21]. To address these shortcomings, researchers have proposed adaptive methods and variable perturbation step sizes to enhance tracking performance and minimize steady state errors [22-23].

To further improve the efficiency and robustness of PV systems, advanced control strategies have been developed, including intelligent MPPT techniques based on Fuzzy logic. FL control offers the advantage of not requiring a mathematical model of the PV system and is effective in managing system nonlinearities. Several alternative nonlinear tracking approaches using fuzzy logic have also been explored in recent studies [24-27].

This study introduces two enhanced Fuzzy Logic (FL) control algorithms FL-Takagi Sugeno and FL-Mamdani designed to improve the efficiency of photovoltaic PV systems while minimizing oscillations around the maximum power point MPP. While Mamdani-based controllers are often limited by design complexity and reliance on heuristic approaches, this work proposes a structured design methodology to overcome the drawbacks associated with classical MPPT techniques, without sacrificing control simplicity.

Unlike traditional fuzzy logic MPPT methods that typically use the error (E) and its change (CE), derived from the power-voltage $P_{pv}(V_{pv})$ curve, this study proposes using the slope and its variation from the power-current $P_{pv}(I_{pv})$ curve as inputs. This alternative approach aims to ensure more precise and stable control under variable conditions.

The proposed PV system, regulated by three MPPT algorithms P&O, IC, and Fuzzy Logic was first simulated in the MATLAB/Simulink environment, operating at a switching frequency of 3900 Hz. The algorithms were then implemented in real time using the low-cost Arduino Mega 2560 platform. Their performance was experimentally validated under steady-state Irradiance (G) and Temperature (T) conditions.

The remainder of this paper is structured as follows: Section 2 presents the components and mathematical modelling of the photovoltaic PV system. Section 3 discusses the design of the DC-DC boost converter. Section 4 describes both classical MPPT techniques, namely Perturb and Observe P&O and Incremental Conductance IC, as well as the development of two fuzzy logic-based controllers. Section 5 provides simulation results for all MPPT strategies using MATLAB/Simulink, while Section 6 presents the experimental validation and performance analysis. The main conclusions and key contributions of this work are summarized in Section 7.

## 2. MATHEMATICAL MODELING OF PHOTOVOLTAIC CELL

The single diode model, characterized by five parameters, is the most widely adopted representation of solar cells [28]. A schematic of this photovoltaic model is illustrated in Figure 1.

The current $I_{pv}$ generated by the photovoltaic cell is expressed as [29] :

$$I_{pv} = I_{ph} - I_s\left[\exp\left(\frac{V_{pv} + I_{pv}R_s}{aV_t}\right) - 1\right] - \frac{V_{pv} + I_{pv}R_s}{R_{sh}} \quad (1)$$

where:

$I_{ph}$: photocurrent
$V_{pv}$: photovoltaic voltage
$R_{sh}$: Shunt Resistance (Ω)
$I_s$: diode saturation current (A)
$R_s$: series resistance (Ω)
a: ideality factor
$V_t$: is defined as KT/q (V)
q: denotes the electric charge of an electron, which is measured at approximately ($1.6\times 10^{-19}$ (C)
T: represents the temperature of the cell measured in Kelvin
K: represents the Boltzmann Constant ($1.38\times 10^{-23}$) (J/K).

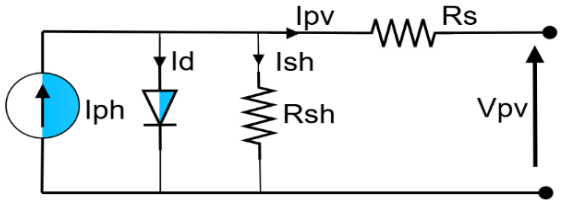


Fig. 1. The equivalent electrical circuit of a photovoltaic (PV) cell single-diode model

Table 1 presents the key parameters of a 50 W PV panel (TDC-P50-42) under standard test conditions [30].

Table 1. PV panel parameter under STC

| Parameter | Value |
|---|---|
| Maximum power ($P_m$) | 50 W |
| Open-circuit voltage ($V_{oc}$) | 24.8 V |
| Short-circuit current (Isc) | 2.7 A |
| Current at the maximum power point ($V_{mpp}$) | 21 V |
| Current at the maximum power point ($I_{mpp}$) | 2.39 A |
| Number of cells | 42 |

The simulation results of the power-current and current-voltage characteristics under various meteorological conditions specifically changes in irradiation at fixed temperature and variable temperature at fixed irradiation level are presented in Figures 2 and 3 respectively.

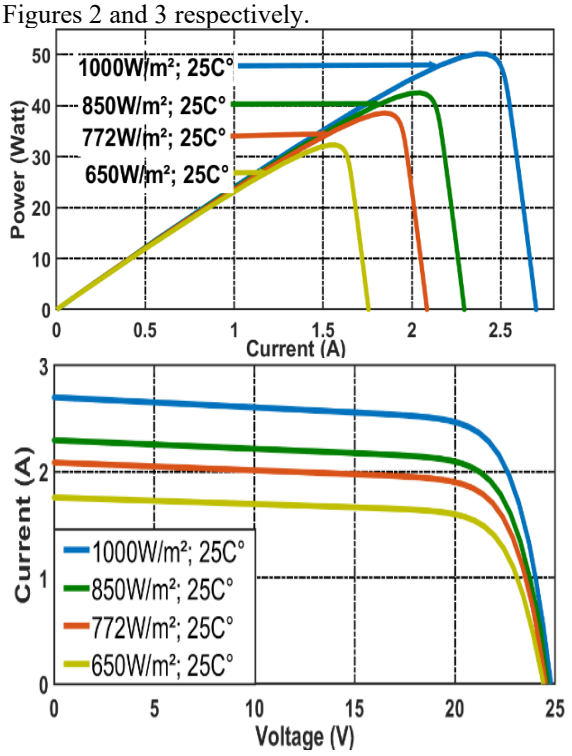


Fig. 2. Power-current and current-voltage curves corresponding to different irradiation levels and a constant temperature value

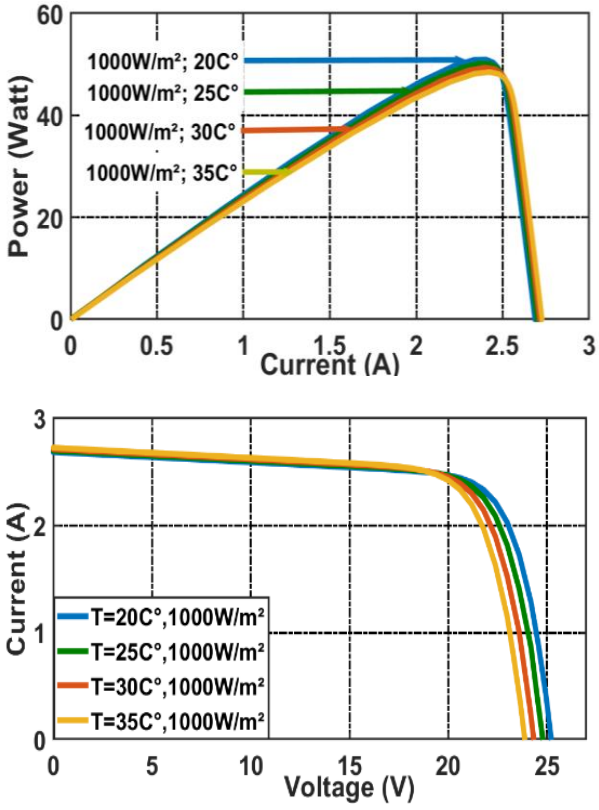


Fig. 3. Power-current and current-voltage curves for various temperature and fixed irradiation values

## 3. PHOTOVOLTAIC SYSTEM

Figure 4 illustrates a schematic diagram of a photovoltaic system. This system includes a 50 W solar panel (TDC-P50-42 delivering power to a resistive load ($R_L$) via a DC-DC boost converter controlled by an MPPT controller. This controller enables automatic tracking of the MPP, thereby ensuring optimal system performance under varying weather conditions and load fluctuations.

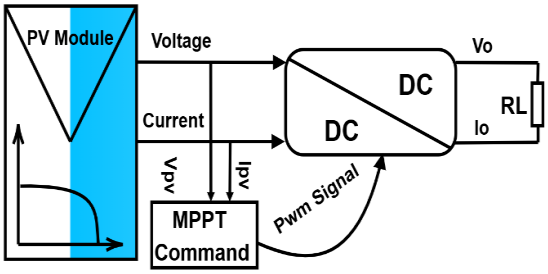


Fig. 4. Schematic representation of the PV system regulated by MPPT command

A Boost-type DC/DC converter is utilized in this study. The electrical connections are established such that the output voltage $V_o$ and output current $I_o$ of the converter are directly linked to the input voltage $V_{pv}$ and current $I_{pv}$ provided by the photovoltaic panel by the following relations [31-34]:

$$V_o = \frac{V_{pv}}{1-D} \quad I_o = I_{pv}\,(1-D) \tag{2}$$

where D is the duty cycle of the PWM signal.

Assuming that the converter operates at (100%) efficiency, the power generated by the photovoltaic panel can be expressed as:

$$P_{pv} = \frac{V_o^2}{R_L} \quad \Longrightarrow \quad P_{pv} = \left(\frac{1}{1-D}\right)^2 \frac{V_{pv}^2}{R_L} \tag{3}$$

Therefore, to extract the maximum power from the PV panel, it is essential to adjust the duty cycle to its optimal value. As illustrated in Figure 5, the DC-DC converter connected to the resistive load $R_L$ can be equivalently modelled as a variable resistance $R_{opt}$, which adapts dynamically to match the panel's optimal operating point.

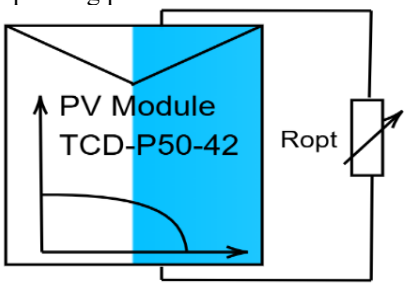


Fig. 5. Synoptic representation of the PV panel connected to the load $R_{opt}$

To achieve effective Maximum Power Point tracking, appropriate load sizing is essential. In continuous conduction mode, the relationship between the actual load resistance $R_L$ and the equivalent optimal resistance $R_{opt}$ can be established

using equation 4, which serves as a key reference for designing the system to operate at its maximum efficiency.

$$\frac{V_{pv}^2}{P_{pv}} = (1-D)^2 R_L \Longrightarrow R_{opt} = (1-D)^2 R_L \quad (4)$$

Thus, the load $R_L$ is expressed as follow:

$$R_L = \frac{R_{opt}}{(1-D)^2} \quad (5)$$

Since:

$$D_{min} < D < D_{max} \quad (6)$$

then:

$$\frac{R_{opt}}{(1-D_{min})^2} \leq R_L \leq \frac{R_{opt}}{(1-D_{max})^2} \quad (7)$$

The optimal resistance $R_{opt}$ required to reach the MPP under Standard Test Conditions is expressed by equation 8:

$$R_{opt} = \frac{V_{mpp}}{I_{mpp}} \quad (8)$$

The results of our analysis indicate that the optimal resistance $R_{opt}$ required to achieve the maximum power point is 8.78 Ω, corresponding to a duty cycle value ranging from 0.2 to 0.89. Within this range, the associated load resistance $R_L$ extends from 13.71 Ω up to 519.52 Ω. Based on these values, a load resistance of 31 Ω was chosen for the system. The detailed specifications of the boost converter components, which ensure operation in continuous conduction mode, are summarized in Table 2 [35-36].

Table 2. PV panel parameter under STC Parameter values for DC/DC boost converter

| Parameters. | Symbol | Value |
|---|---|---|
| Input Capacitor [µF] | Ce | 1000 |
| Inductance [µH] | L | 195 |
| Output capacitor [µF] | Cs | 1000 |

## 4. PROPOSED MPPT COMMAND

This study explores and compares three MPPT control strategies: the classical P&O and IC algorithms, and the proposed Fuzzy Logic based controller FL-Mamdani and FL-Takagi-Sugeno. Each method presents specific advantages and limitations regarding efficiency, implementation simplicity, robustness, and dynamic response. The comparative analysis is conducted under varying irradiance conditions to evaluate the effectiveness of each technique in accurately and reliably tracking the maximum power point.

### 4.1. P&O Perturbation and Observation

Perturbation and Observation MPPT control is thought to be among the most extensively used classical algorithms.

The principle of this method is to perturb the PV panel voltage; therefore, the output PV power will be perturbed. If the PV power increases, i.e., it is higher than the old one, it means that the operating point is moving towards the MPP and the duty cycle change should be maintained in the same direction until the maximum power is reached ($dP_{pv}/dV_{pv} = 0$). Otherwise, if the power decreases, the operating point moves away from the MPP. So, the direction of the perturbation to reach the maximum power must be changed. Figure 6 illustrates the flowchart of the P&O algorithm [29].

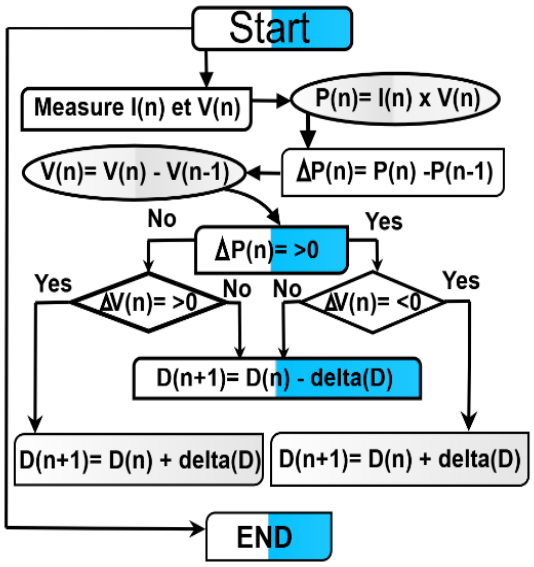


Fig. 6. P&O flowchart algorithm

### 4.2. Incremental Conductance Control

The IC algorithm relies on the slope of the photovoltaic power-voltage curve, described by the following Equation:

$$\frac{dP_{PV}}{dV_{PV}} = 0 \quad (9)$$

Equation 9 can be expressed as below:

$$\frac{dP_{PV}}{dV_{PV}} = I_{PV} + V_{PV}\left(\frac{dI_{PV}}{dV_{PV}}\right) \quad (10)$$

At MPP:

$$\left(\frac{dP_{PV}}{dV_{PV}}\right)_{MPP} = 0 \Longrightarrow \frac{dI_{PV}}{dV_{PV}} + \frac{I_{PV}}{V_{PV}} = 0 \quad (11)$$

At the operating points illustrated in Figure 7, the IC algorithm regulates the system by decreasing the voltage when $dP_{PV}/dV_{PV} < 0$ and increasing it when $dP_{PV}/dV_{PV} > 0$.

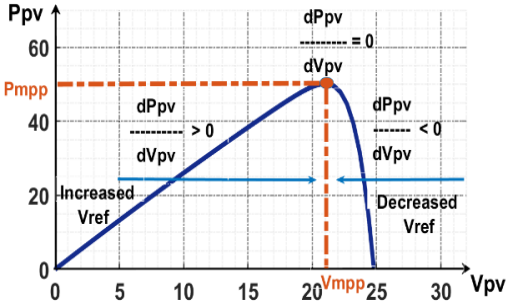


Fig. 7. Power - voltage characteristic

As illustrated in the flowchart of the Incremental Conductance IC algorithm given in Figure 8, the

control strategy evaluates the photovoltaic voltage V(k) and current I(k) at each sampling instant k. It subsequently calculates the conductance $I_{PV}/V_{PV}$ and the incremental conductance $dI_{PV}/dV_{PV}$. Based on these values, the algorithm identifies the maximum power point on the PV curve using the following set of equations:

$$\frac{dP_{PV}}{dV_{PV}} = 0 \implies \frac{dI_{PV}}{dV_{PV}} = -\frac{I_{PV}}{V_{PV}} \quad (12)$$

$$\frac{dP_{PV}}{dV_{PV}} > 0 \implies \frac{dI_{PV}}{dV_{PV}} > -\frac{I_{PV}}{V_{PV}} \quad (13)$$

$$\frac{dP_{PV}}{dV_{PV}} < 0 \implies \frac{dI_{PV}}{dV_{PV}} < -\frac{I_{PV}}{V_{PV}} \quad (14)$$

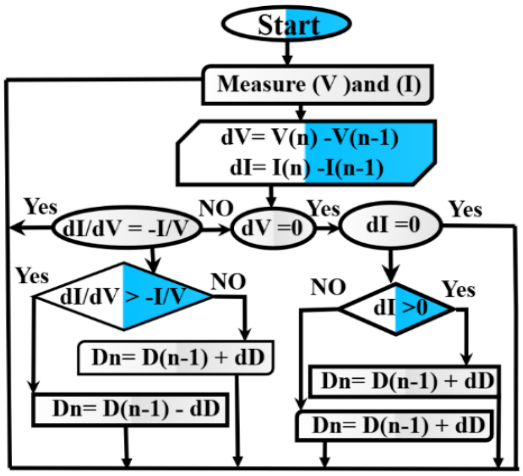


Fig. 8. Flowchart outlining the IC algorithm

### 4.3. Fuzzy logic MPPT command

The Fuzzy Logic MPPT Controller is a technique used to enhance the efficiency of nonlinear systems, such as photovoltaic systems. This method involves three main stages: Fuzzification, Inference, and Defuzzification, as illustrated in Figure 9.

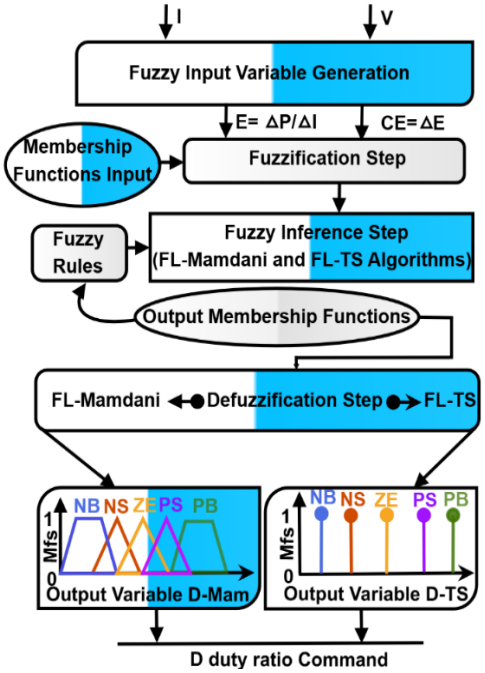


Fig. 9. Flowchart illustrating the operation of a FL commands

The proposed MPPT control approach in this study employs the error E and the change in error CE as input variables, which represent the slope and the variation of the slope of the power-current P(I) characteristic curve, respectively. Based on these inputs, the controller generates an appropriate D to drive the Mosfet of the DC-DC converter, thereby ensuring maximum power transfer from the photovoltaic panel to the load. As demonstrated in the following section, this method significantly enhances the performance of the photovoltaic system under varying environmental conditions.

The Fuzzification process involves converting the crisp input values E and CE into linguistic fuzzy variables. At a given time t, these input variables are defined as shown in Eqs. (15):

$$E(t) = \frac{P(t) - P(t-1)}{I(t) - I(t-1)} \quad (15)$$

$$CE(t) = E(t) - E(t-1)$$

Where P(t) and I(t) stand for the solar panel's power and current, respectively. Five linguistic variables or labels are used to represent the input variables, E and CE, which are stated as follows:

- **NB**: Negative-big,
- **NS**: Negative-small,
- **ZE**: Zero,
- **PB**: Positive-big,
- **PS**: Positive-small.

Various types of fuzzy Membership functions (MFs) can be utilized in the Fuzzification process, including triangular, trapezoidal, and Gaussian shapes. The selection of a specific MFs shape typically depends on expert knowledge and prior experience with the system. Among these, triangular and trapezoidal functions are commonly preferred due to their simplicity and effectiveness in delivering reliable results. The standard Membership functions used for both the input and output variables in the Fuzzification process are depicted in Figure 10.

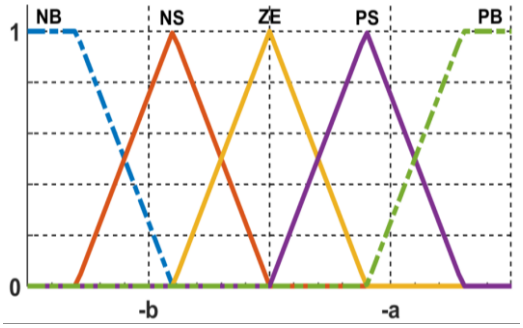


Fig. 10. Typical Fuzzy membership functions (MFs) of inputs and output used in the fuzzification process

During the Inference step, the Fuzzy Logic controller establishes a relationship between the input and output linguistic variables using a predefined rule base, as illustrated in Table 3. This rule base must account for both the static and dynamic characteristics of the controlled system. The Inference mechanism enables decision making by applying fuzzy rules to the fuzzified inputs. For

example, if the E is classified as Negative Big (NB) and the CE is also NB, then the output duty cycle is assigned a linguistic value of Zero (ZE).

Table 3. Fuzzy rules that establish relationships between output and inputs variables

| (CE) / (E) | NB | NS | ZE | PS | PB |
|---|---|---|---|---|---|
| NB | ZE | ZE | NB | NB | NB |
| NP | ZE | ZE | NS | NS | NS |
| ZE | NS | ZE | ZE | ZE | PS |
| PS | PS | PS | PS | ZE | ZE |
| PB | PB | PB | PB | ZE | ZE |

The Defuzzification step is the final stage of the Inference process in a fuzzy logic system. It consists to defuzzify the D output fuzzy set of the Mamdani and TS fuzzy Inference system. Which means converting the fuzzy output obtained from the fuzzy rules into a numerical value.

In this work, we use two types of Fuzzy Logic controls: The FL-Mamdani algorithm and the FL-TS method.

The FL-Mamdani system which is the most commonly used is based on centroid Defuzzification method. This method returns the numerical value of the D output. The center of gravity is calculated by weighting the values of the fuzzy outputs by their degree of membership, adding them together, and then dividing the result by the sum of the degrees of membership. Conversely, the FL-TS method employs a weighted average approach to ascertain the output D. Unlike representing the output as a fuzzy set, it is expressed as a constant or a linear equation. The MFs of the E: inputs and CE, along with the output D, are illustrated in Figures. 11 to 13 for both the FL- Mamdani and FL-TS methods.

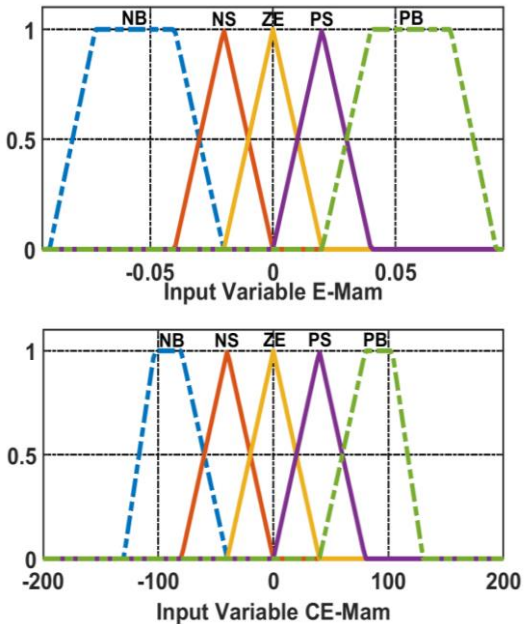


Fig. 11. MFs of the inputs E and CE for FL-Mamdani

Figure 14 shows the output surface for the fuzzy Inference system for both the FL-Mamdani and FL-TS MPPT commands used to control PV system. It represents the output variable (D) against the two input variables (E, CE).

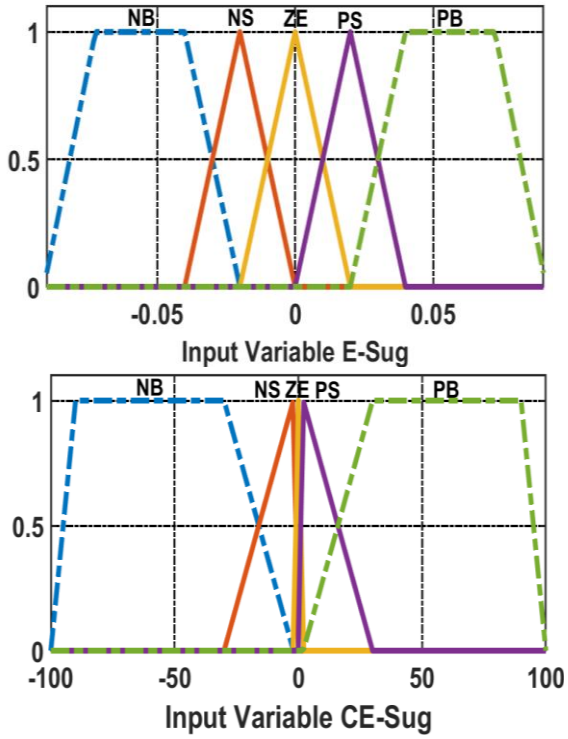


Fig. 12. MFs (E) and (CE) inputs for FL-TS

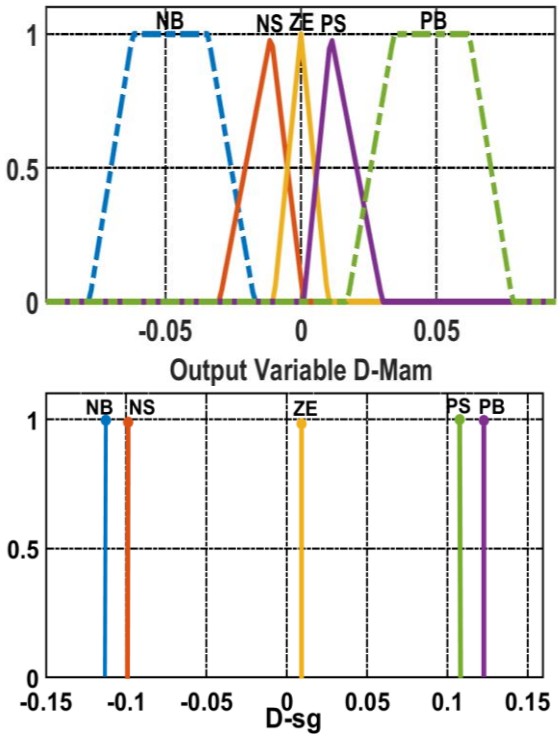


Fig. 13. Membership functions (MFs) for the output D in FL-Mamdani and FL-TS

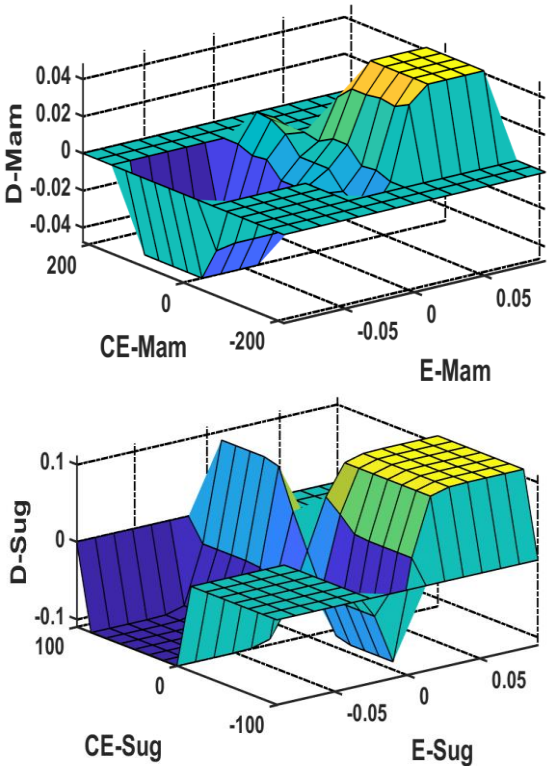


Fig. 14. Output surface MPPT control methods of FL-Mamdani and FL-TS

## 5. RESULTS OF SIMULATION

This section presents the simulation results of the proposed photovoltaic system using the Matlab/Simulink environment. The system architecture comprises a photovoltaic panel, a boost converter, an MPPT controller, and a resistive load. Experimental tests were conducted to evaluate system performance under varying environmental conditions, specifically at an irradiance level of 772 W/m² and a temperature (T) of 25 °C. Figure 15 illustrates the different test conditions used in the study. To ensure the validity and robustness of the developed Fuzzy Logic MPPT tracker, a comparative assessment was performed between conventional controllers P&O, IC and the two proposed FL controllers FL-Mamdani and FL-TS under the irradiance profiles shown in Figure 15, while maintaining a constant temperature of 25 °C.

The results illustrated in Figures 16 and 17 demonstrate that the proposed MPPT controllers namely P&O, IC, and Fuzzy Logic controllers FL-Mamdani and FL-TS integrated with the boost converter, effectively accomplish their intended objectives. These include increasing the output voltage, reducing the current, and ensuring efficient power transfer at the maximum power point Pmax from the photovoltaic panel to the load, as evidenced by the profiles in Figure 17. Notably, the duty cycle is precisely regulated to match the MPP, with the FL-TS method exhibiting the highest accuracy.

Moreover, the Fuzzy Logic controllers significantly reduce oscillations around the MPP compared to the conventional P&O and IC algorithms. These findings indicate that FL controllers offer superior performance in terms of accuracy and stability. Furthermore, they exhibit faster dynamic responses, with response times of 28.15 ms for FL-Mamdani and 22.01 ms for FL-TS, compared to 48.02 ms for P&O and 40.25 ms for IC. This makes Fuzzy Logic MPPT methods, particularly FL-TS, more suitable for real-time photovoltaic energy optimization under varying environmental conditions.

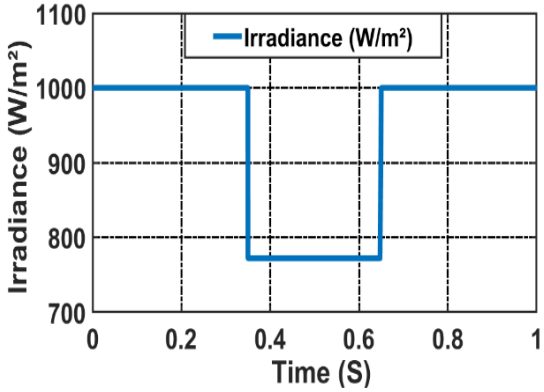


Fig. 15. Sudden change in irradiation levels (G)

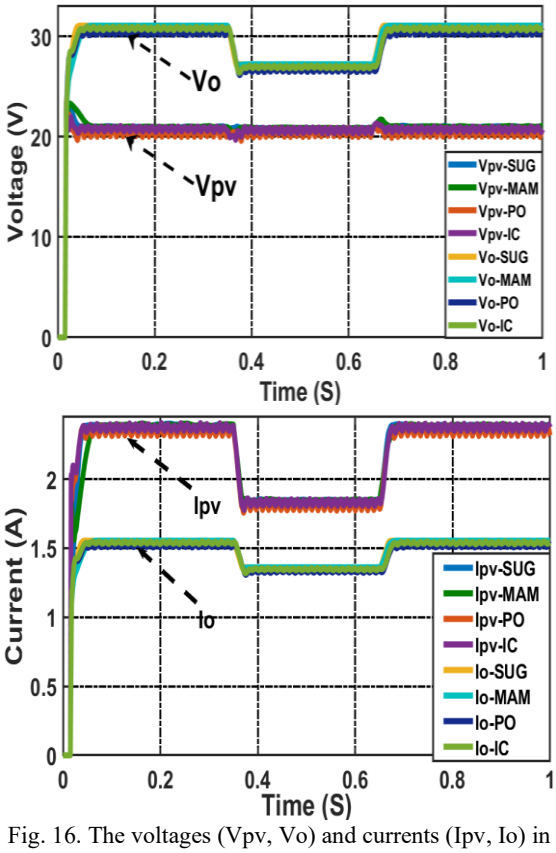


Fig. 16. The voltages (Vpv, Vo) and currents (Ipv, Io) in terms of input and output of converter boost controlled by (IC, P&O and Fuzzy Logic) MPPT controls according to the rapid change in G level

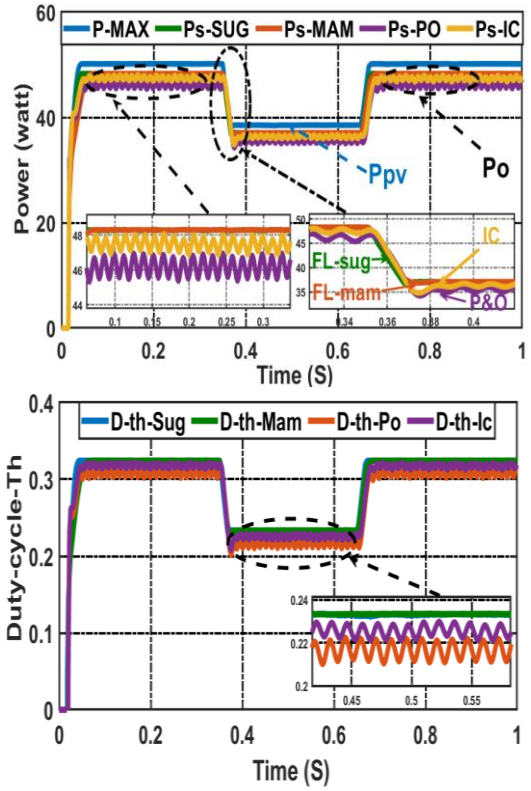


Fig. 17. Output Powers (Pmax; Ps) and duty cycle (D) of converter boost controlled by (P&O and Fuzzy Logic) MPPT controls according to the rapid change in irradiation level

## 6. EXPERIMENTAL RESULTS AND DISCUSSIONS

### 6.1. Description of experimental test bench

This section presents the practical validation of the implemented MPPT algorithms, including Fuzzy Logic methods FL-Mamdani and FL-TS and conventional techniques IC and P&O, using the Simulink Support Package for Arduino hardware.

The experimental setup, shown in Figure 18, integrates both hardware and software components to enable real time testing and evaluation of the control strategies.

- ✓ A PV module of 50 W under STC, a boost converter, and a resistive load.
- ✓ An Arduino Mega 2560.
- ✓ Instruments for measurement and acquisition include a watt-meter and an oscilloscope.
- ✓ A personal computer utilizing the Matlab-Simulink environment.

### 6.2. Description of hardware

Arduino Mega 2560, which uses the ATmega2560 microcontroller. 4 UART (hardware serial ports), 16 analogue inputs, a 16 MHz crystal oscillator, USB connection, power jack, ICSP header and reset button are included related to digital input-output pins were now totalling its count as 54 but compared with Arduino Uno Atmega168 Darlington.

We prepared an electronic interface card to allow the collection of ($I_{PV}$) and ($V_{PV}$) from one PV panel and for the control of a DC-DC boost converter. In order to prevent Arduino Mega 2560 from experiencing operational issues, it is important that the main board isolate an opto-coupler with respect to power circuit.

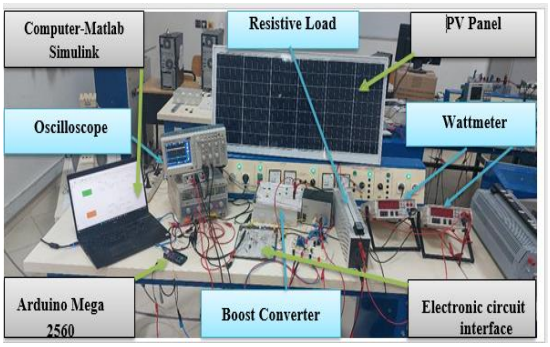


Fig. 18. Experimental test bench of the PV system

In the experimental test bench of Fig. 18, the LEM LA-55-P sensor was used for current measurement, as it is specifically calibrated to provide exact current measurements in the range of [0A to 5A]. The C11A063 sensor module based on the resistance point pressure principle is used to measure the voltage of the photovoltaic panel. It can reduce the input voltage up to five times.

The (HCPL-3120) optically linked driver was used to isolate and drive the gate of a metal oxide semiconductor field effect transistor Mosfet. The DC-DC converter, positioned between the photovoltaic panel and the load operates at a designed switching frequency of 3900 (Hz). This converter incorporates a Schottky diode and an IRF740 Mosfet, which was chosen for its high performance in our system. Figure 18. depicts the experimental test bench used to carry out the essential experiments to validate our system.

### 6.3. Description of the software

The aim of this research is to create and implement a real-time MPP tracker by leveraging the Matlab-Simulink environment in conjunction with the Arduino Mega 2560 board.

This method is regarded appropriate since it combines a solid performance prototyping board with effective simulation software. The Simulink/Support/Package for Arduino Hardware from Matlab-Simulink enables the design of control algorithms directly in Simulink, which can then be down loaded onto the Arduino board hardware platform. Figure 19. provides a glimpse of the interface developed within the Matlab Simulink environment, utilized for the real time implementation of MPPT commands (IC, P&O, FL).

Both conventional MPPT techniques Perturb and Observe and Incremental Conductance as well as the Fuzzy Logic controller, rely on two essential input parameters: the photovoltaic current Ipv and voltage $Vpv$. These inputs are critical for accurately determining the operating point of the PV system. In the implementation, Simulink blocks illustrated in

Figure 19 are employed to compute these values based on real time data received from the photovoltaic panel.

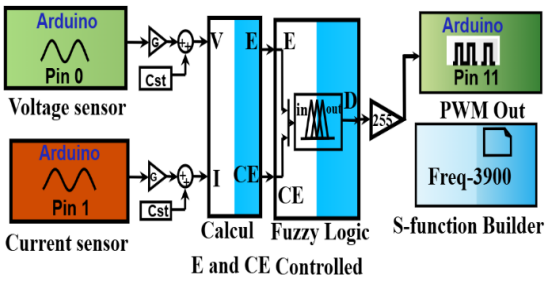


Fig. 19. View of interface developed in Matlab/Simulink environment for real- time implementation of FL MPPT command

The current and voltage sensors are linked to the Arduino Mega 2560 board's analogue pins [A0 and A1], respectively. The algorithm generates a D that regulates the PWM block using a gain of 255. The Pulse Width Modulation target accepts only integer values between 0 and 255, corresponding to 0% to 100%. Once the Arduino Mega 2560 board is connected to the computer via a USB cable and configured, the model can be deployed onto the Arduino hardware. Output block in the Simulink-Support Package generates a maximum frequency of 490 Hz, which is unsuitable for driving the boost converter DC/DC. To address this limitation, Matlab S-functions are employed. To adjust the frequency, we propose integrating Matlab S-functions with the control governing the PWM boost frequency in the Simulink model.

An S-function block in Matlab/Simulink enables the integration of C code directly into a Simulink model, offering flexibility in real-time control applications. In this study, an S-function is employed to implement a control algorithm that achieves a switching frequency of 3900 Hz, ensuring accurate and high-speed regulation of the DC-DC boost converter. We use for this the following C command [37]:

TCCR1B = (TCCR1B & 0 X F8 | 0 X 02)

It should be noted that Arduino Mega 2560 board features 14 PWM outputs managed by three timers. The PWM frequency is determined by the timer clock, which runs at 62,500 Hz divided by a prescaler. To obtain a PWM frequency of approximately 3.9 kHz, the base frequency must be divided by 16 (i.e., 62,500 / 16 ≈ 3906 Hz). This is achieved by setting the prescaler of Timer1 to 8, using Previews C command.

### 6.4. Experimental results

To determine the Maximum Power Point under experimental conditions at a given moment, a preliminary test was conducted. By varying the converter's duty cycle from 0 to 1, the system is guaranteed to pass through the MPP. This procedure was implemented using a simple algorithm programmed on the Arduino board, which progressively increases the duty cycle of the PWM signal from 0 to 1. During this process, a digital oscilloscope is employed to monitor and verify the power output from the photovoltaic panel, ensuring accuracy in power tracking, as illustrated in Figure 20. The resulting PV characteristics, shown in Figure 21, reveal that the MPP under these specific conditions is approximately 44.22 W.

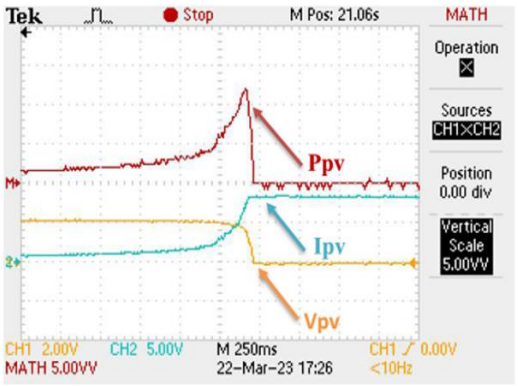


Fig. 20. $\mathbf{I_{PV}}(t)$, $\mathbf{V_{PV}}(t)$ and $\mathbf{P_{PV}}(t)$ characteristics

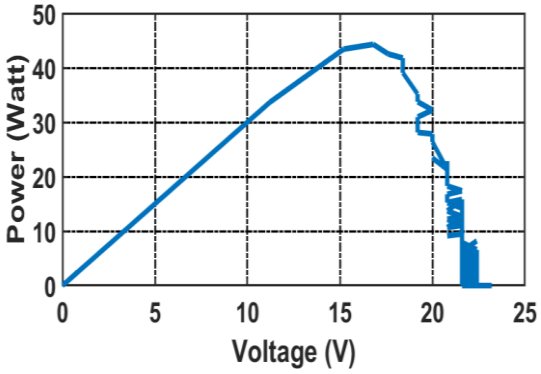


Fig. 21. Experimental power-voltage characteristics

The conducted experiments aim to evaluate the performance of Fuzzy Logic controllers specifically FL-Mamdani and FL-TS in comparison with conventional MPPT methods, namely Perturb and Observe and Incremental Conductance. All evaluations are carried out under identical operating conditions, with a switching frequency set at 3900 Hz.

### 6.5. Results for classical controls

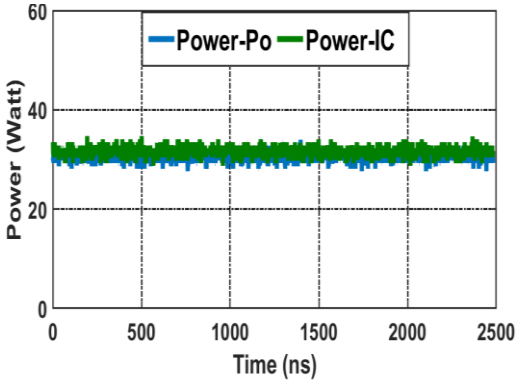


Fig. 22. Waveforms of PV power Ppv in the case of Boost converter controlled by (P&O or IC) MPPT command

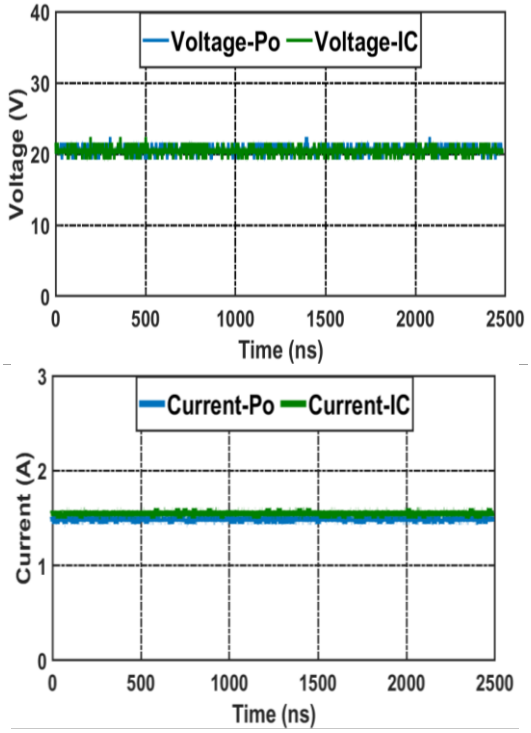


Fig. 23. Waveforms of Vpv voltage and Ipv current in the case of Boost converter controlled by (P&O or IC)

### 6.6 Results for fuzzy-logic controls

Figures 24, 25, and 26 illustrate the power, current, and voltage outputs of the photovoltaic panel when controlled by FL-Mamdani and FL-TS MPPT techniques, respectively. Under consistent test conditions, these results confirm the experimental validity of the applied MPPT algorithms. The power profiles clearly demonstrate that fuzzy logic controllers outperform conventional methods (P&O and IC), particularly in steady-state performance, by significantly reducing oscillations around the maximum power point. Moreover, the power extracted using FL-Mamdani and FL-TS controllers exceeds that achieved by the P&O and IC techniques, as evidenced across Figures 22 to 23.

Switching losses are one of the main challenges associated with power converters. In this study, the power, voltage, and current values measured at the output of the boost converter using Fuzzy Logic MPPT controllers are as follows: for the FL-TS controller, the power is 38.5 W, the voltage is 20.32 V, and the current is 1.89 A; for the FL-Mamdani controller, the power is 37.8 W, the voltage is 20.36 V, and the current is 1.86 A. These results highlight the effectiveness of Fuzzy Logic control in minimizing energy losses. In our case, the efficiency of the DC-DC boost converter is approximately 85%.

Figures 27 and 28 show the PWM control signals of the boost converter for all controls, indicating a Duty cycle of 20.12% and a frequency of 3900 (Hz).

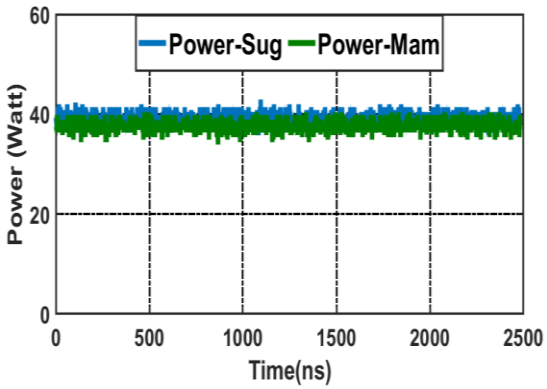


Fig. 24. Waveform of PV power Ppv in the case of DC-DC converter controlled by (FL-Mamdani or FL-Takagi Sugeno) MPPT command

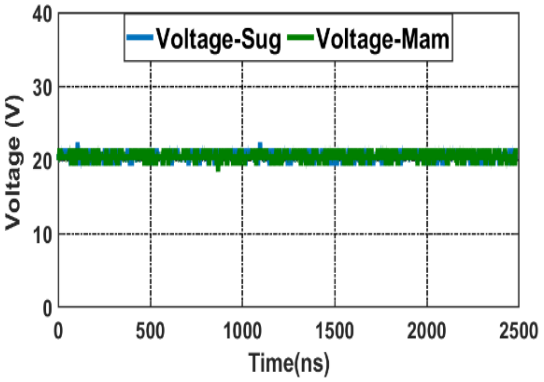


Fig. 25. Waveform of voltage (Vpv) in the case of DC-DC converter controlled by (FL-Mamdani or FL-TS) MPPT command

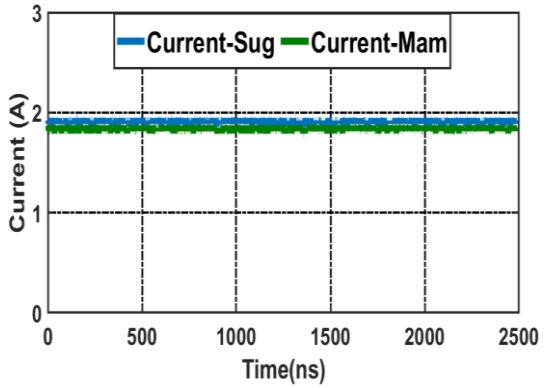


Fig. 26. Waveform of current (Ipv) in the case of DC-DC converter controlled by (FL-Mamdani or FL-TS) MPPT command

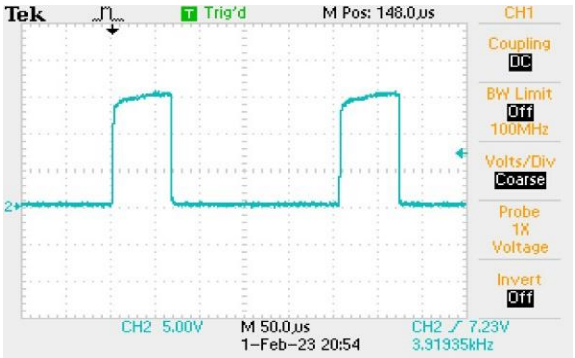


Fig. 27. PWM Signal for Fl-Mamdani Control

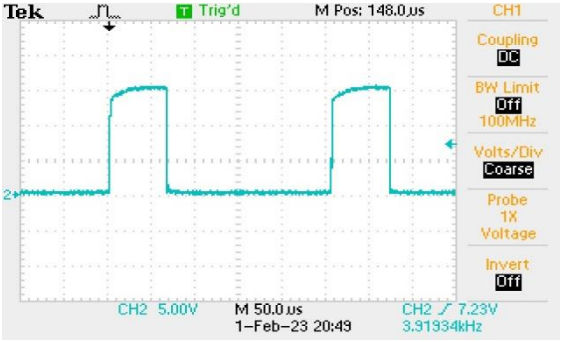


Fig. 28. PWM Signal for FL-TS Control

## 7. CONCLUSION

This article introduces and thoroughly investigates a novel MPPT control strategy based on enhanced Fuzzy Logic algorithms, specifically FL-Mamdani and FL-TS, which leverage inputs derived from the slope of the power-current P(I) curve and its variations. This innovative approach contrasts with conventional MPPT techniques that utilize the slope of the power-voltage P(V) curve. The study offers a comprehensive comparative analysis between this proposed method and classical MPPT algorithms Perturb and Observe P&O and Incremental Conductance IC through simulations in Matlab-Simulink and real-time hardware implementation using the Arduino Mega 2560.

The proposed Fuzzy Logic controllers demonstrated superior performance in reducing oscillations around the MPP and exhibited significantly faster convergence times 22.01 ms for FL-TS and 28.15 ms for FL-Mamdani compared to 48.02 ms for P&O and 40.25 ms for IC. These results were consistent across various irradiance conditions, confirming the robustness and efficiency of the approach.

In conclusion, the FL-TS MPPT algorithm emerges as an effective and practical solution for photovoltaic system control, ensuring optimal energy extraction through rapid and accurate tracking of the MPP. This innovative method represents a significant advancement in MPPT techniques and offers promising applications for enhancing solar energy harvesting.

**Source of funding:** *This research received no external funding.*

**Author contributions:** *research concept and design, M.B., Y.K.; Collection and/or assembly of data, M.B., M.L.E.; Data analysis and interpretation, M.B., Y.K.; Writing the article, M.B.; Critical revision of the article, M.B., Y.K., M.L.E.; Final approval of the article, M.B.*

**Declaration of competing interest:** *The authors declare that they have no known competing financial interests or personal relationships that could have appeared to influence the work reported in this paper.*

## REFERENCES

1. An L, Dylan L. Design of a single-switch DC/DC converter for a PV-battery-powered pump system with PFM+PWM control. IEEE Transactions on Industrial Electronics. 2015;62(2):910-921. https://doi.org/10.1109/TIE.2014.2359414.
2. Ibrahim EH, Aslan SR. Solar photovoltaic water pumping system approach for electricity generation and irrigation: Review. Diagnostyka. 2023;24(2): 2023211. https://doi.org/10.29354/diag/165849.
3. Aashoor FAO; Robinson FVP. Maximum power point tracking of photovoltaic water pumping system using fuzzy logic controller. Proceedings of the Universities Power Engineering Conference. 2013:1-5. https://doi.org/10.1109/UPEC.2013.6714969.
4. El Idrissi R, Abbou A, Mokhlis M, Salimi M. A comparative study of MPPT controllers for photovoltaic pumping system. 9th International Renewable Energy Congress (IREC). 2018:1-6. https://doi.org/10.1109/IREC.2018.8362524.
5. Aldjia L, Kesraoui M, Djalloul A. Energy management and control of a hybrid water pumping system with storage. Applied Solar Energy, Appl. Sol. Energy. 2017;53:190-198. https://doi.org/10.3103/S0003701X17020025.
6. Zaid SA, Albalawi H, Alatawi KS, El-Rab HW, El-Shimy ME, Lakhouit A, Alhmiedat TA, Kassem AM. Novel fuzzy controller for a standalone electric vehicle charging station supplied by photovoltaic energy. Appl. Syst. Innov. 2021;4:63. https://doi.org/10.3390/asi4030063.
7. Raturi, A. Feasibility study of a solar water pumping system. Appl. Sol. Energy. 2011;47:11-13. https://doi.org/10.3103/S0003701X11010129.
8. Nasri E, Jarou T, Benchikh S, Elkoudia Y. Reliable energy supply and voltage control for hybrid microgrid by pid controlled with integrating of an EV charging station. Diagnostyka. 2023;24(4):2023409. https://doi.org/10.29354/diag/174145.
9. Po-Cheng Chen PYC, Yi-Hua L, Jing-Hsiao C. A comparative study on maximum power point tracking techniques for photovoltaic generation systems operating under fast-changing environments. Sol. Energy. 2015;119:261-276. https://doi.org/10.1016/j.solener.2015.07.006.
10. Lalouni S, Rekioua D, Rekioua T. Matagne E. Fuzzy logic control of stand-alone photovoltaic system with battery storage. Journal of Power Sources. 2009;193: 889-907. https://doi.org/10.1016/j.jpowsour.2009.04.016.
11. Bounechba H, Bouzid A, Nabti K, Benalla H. Comparison of perturb & observe and fuzzy logic in maximum power point tracker for PV systems. International Journal Energy Procedia. 2014;50:667-684. https://doi.org/10.1016/j.egypro.2014.06.083.
12. Doudou NL, Atanda KR. Comparing fuzzy rule-based MPPT techniques for fuel cell stack applications, Journal Energy Procedia. 2019;156:177-182. https://doi.org/10.1016/j.egypro.2018.11.124.
13. Gupta A, Chauhan YK, Pachauri RK. A comparative investigation of maximum power point tracking methods for solar PV system. Solar Energy. 2016;136: 236-253. https://doi.org/10.1016/j.solener.2016.07.001.
14. Motahhir S, El Hammoumi A, El Ghzizal A. Photovoltaic system with quantitative comparative

between an improved MPPT and existing INC and P&O methods under fast varying of solar irradiation. Energy Reports. 2018;4:341-350. https://doi.org/10.1016/j.egyr.2018.04.003.
15. Gupta AK, Chauhan YK, Maity T. Experimental investigations and comparison of various MPPT techniques for photovoltaic system. Indian Academy of Sciences. 201843:4-15. https://doi.org/10.1007/s12046-018-0815-0.
16. Sellami A, Kandoussi K, El Otmani R, Eljouad M, Mesbahi O, Hajjaji A. A novel auto scaling MPPT algorithm based on perturb and observe method for photovoltaic modules under partial shading conditions. Appl. Sol. Energy. 2018;54:149-158. https://doi.org/10.3103/S0003701X18030143.
17. Loukriz A, Haddadi M, Messalti S. Simulation and experimental design of a new advanced variable step size Incremental Conductance MPPT algorithm for PV systems, , Journal ISA Transactions. 2016;62:30-38. https://doi.org/10.1016/j.isatra.2015.08.006.
18. Kamal S, Aniket A, Anjanee Kumar M, Bhim S, Kaldeep, S. SEPIC converter for solar PV array fed battery charging in DC homes; Journal of The Institution of Engineers (India) Transactions. 2021; 102:455-463. https://doi.org/10.1007/s40031-020-00522-0.
19. Rokeya JM, Ariful I. Modeling and performance analysis of PV module with Maximum Power Point Tracking in Matlab/Simulink. Applied Solar Energy. 2015;51:245-252. https://doi.org/10.3103/S0003701X15040155.
20. Farayola AM, Hasan AN, Ali A. Implementation of modified incremental conductance and fuzzy logic MPPT techniques using MCUK converter under various environmental conditions. Appl. Sol. Energy. 2017;53:173-184. https://doi.org/10.3103/S0003701X17020050.
21. Mukti RJ, Islam A. Modeling and performance analysis of PV module with maximum power point tracking in Matlab/Simulink. Appl. Sol. Energy. 2015; 51:145-252. https://doi.org/10.3103/S0003701X15040155.
22. Yamina K, Hajji B, Adel M. A new maximum power point tracking PV control for rapid changes in irradiation level. Proceedings of the 1st International Conference on Electronic Engineering and Renewable Energy. 2019;512:384-391. https://doi.org/10.1007/978-981-13-1405-6_46.
23. Yuncong J, Qahouq JA, Haskew TA. Adaptive step size with adaptive- perturbation-frequency digital MPPT controller for a single-sensor photovoltaic solar system. IEEE Transactions on Power Electronics. 2013;28:3195-3205. https://doi.org/10.1007/978-981-13-1405-6_46.
24. Ahmed KA, Ahmed MM, Shehab A, Parasad NE, High-peformance adaptive perturb and observe MPPT technique for photovoltaic-based micro-grids. IEEE Transactions on Power Electronics. 2011;26(4):1010-1021. https://doi.org/10.1109/TPEL.2011.2106221.
25. Bhukya L, Nandiraju S, Messaoudi A. A novel photovoltaic maximum power point tracking technique based on grasshopper optimized fuzzy logic approach. International Journal of Hydrogen Energy. 2020;45:9416-9427. https://doi.org/10.1016/j.ijhydene.2020.01.219.
26. Rezk H, Aly M, Al-Dhaifallah M, Shoyama M. Design and hardware implementation of new adaptive fuzzy logic-based MPPT control method for photovoltaic appli-cations. IEEE Access. 2019;7:106427-106438. https://doi.org/10.1109/ACCESS.2019.2932694.
27. Mohammed B, Yamina K, Bekkay H. Efficient fuzzy logic MPPT controls for sudden change in load. Lecture Notes in Electrical Engineering. 2023. https://doi.org/10.1007/978-981-19-6223-3_50.
28. Ouahib G, Dahhou B, Ferhat, C, Adaptive fuzzy controller based MPPT for photovoltaic systems. Journal Energy Conversion and Management. 2014; 78:843-850. https://doi.org/10.1016/j.enconman.2013.07.093.
29. Saad M, Abdelaziz EG, Souad S, Aziz D. Modeling of photovoltaic system with modified incremental conductance algorithm for fast changes of irradiance. International Journal of Photoenergy. 2018:1-3. https://doi.org/10.1155/2018/3286479.
30. Mohammed B, Bekkay B, Hassan M, Khalid C. Neural network-based precision irrigation scheduling and crop water stress index (CWSI) Assessment in book: Proceedings of the 3rd International Conference on Electronic Engineering and Renewable Energy Systems. 2023:661-669. https://doi.org/10.1007/978-981-19-6223-3_68.
31. Aicha D, Mohamed MR, Ali, T, Mohamed B. The MPPT command for a PV system comparative study: control based on fuzzy logic with P&O. Renewable Energy for Smart and Sustainable Cities. 2019;62: 346-354. https://doi.org/10.1007/978-3-030-04789-4_38.
32. Unal Y, Ali K, Selim B. PV system fuzzy logic MPPT method and PI control as a charge controller. Renewable and Sustainable Energy Reviews. 2018;81: 994-1001. https://doi.org/10.1016/j.rser.2017.08.048.
33. Yamina K, Aziz A. Efficient energy utilization of standalone photovoltaic system under rapid change in load. AIP Conference Proceedings. 2018;2056:SP-0200026. https://doi.org/10.1063/1.5084999.
34. Mohammed B, Yamina K, Anas B, Mohamed LHA. Optimization of photovoltaic system using Mamdani and Takagi Sugeno MPPT Controls. 2022 2nd International Conference on Innovative Research in Applied Science, Engineering and Technology (IRASET). 2022:1-5. https://doi.org/10.1109/IRASET52964.2022.9738070.
35. Abdellahi B, Ould Ehssein C, Mahmoud M, Hamdoun O, Elhassen A. Comparative study of different DC/DC power converter for optimal PV system using MPPT (P&O) Method. Appl.Sol. Energy. 2018;54:235-145. https://doi.org/10.3103/S0003701X18040047.
36. Benbitour Khennane M, Boughali S, Bechki D, Zaghba L, Fezzani A, Hadj Mahammed I. Experimental performance characterization and economic efficiency of 16.28 kWp grid-tied PV systems in semi-arid climate. Diagnostyka. 2021;22(2):53-65. https://doi.org/10.29354/diag/135926.
37. Mohamed F, Mohamed LH, Mohamed Z, Mohamed LHA. Hardware implementation of the fuzzy logic MPPT in an Arduino card using a Simulink Support Package for photovoltaic application. IET Renewable Power Generation. 2018:13. https://doi.org/10.1049/iet-rpg.2018.%205667.

**Mohammed BOUTAYBI** earned his Master's degree in Physics with a specialization in Mechanics and Energetics from the Faculty of Sciences in Oujda, Morocco, in 2019. Presently, he is pursuing a Ph.D. at the National School of Applied Sciences in Oujda. His research interests primarily focus on artificial intelligence applications across various domains, including embedded systems and power electronics.
e-mail: mohammed.boutaybi@ump.ac.ma

**Yamina KHLIFI**
e-mail: khlifi_yamina@yahoo.fr

**Mohamed Larbi ELHAFYANI**
e-mail: m.elhafyani@ump.ac.ma